Online-Journals.org

iJET International Journal of Emerging Technologies in Learning

iJET | eISSN: 1863-0383 | Vol. 18 No. 22 (2023) | OPEN ACCESS

https://doi.org/10.3991/ijet.v18i22.44097

PAPER

Practical Analysis of Digital Technology in an Electronic Education Platform in PE Training

Qiyu Luo(✉)

College Office, Hunan Sports Vocational College, Changsha, China

Qiyu_Luo@outlook.com

ABSTRACT

To improve the practical effect of digital technology (DT) in electronic education platform (ECP) in sports training, this study proposes using OpenPose as the main method of posture matching in sports teaching. MobileNet was introduced to replace the backbone network in OpenPose to improve the efficiency of the model. At the same time, self-attention mechanism (SAM) is introduced to improve the accuracy of the model. In the performance verification results, the proposed algorithm has a mean mean absolute error (MAE) of 0.793 and a root mean square error (RMSE) of 0.628. The accuracy of the proposed algorithm reached a maximum of 0.893 in the test set. The accuracy of the proposed algorithm exceeds 90% in the training set. In the practice of physical education (PE) and training, the absolute error between the actual value and the predicted value does not exceed 1.5 cm, while the relative error does not exceed 1.2%. The minimum absolute error and relative error are 0.01 cm and 0.2%, respectively. The proposed algorithm has high prediction effect and performance, and can be applied to PE training.

KEYWORDS

electronic education platform (ECP), digital technology, physical education (PE), OpenPose, MobileNet, self-attention mechanism (SAM)

1 INTRODUCTION

The development of digital technology (DT) has promoted the rapid dissemination of network resources. In the field of education, the application of DT has promoted the establishment of an electronic education platform (ECP) [1]. In the teaching of physical education (PE), action demonstration and action imitation are important forms of physical education teaching. For physical education teaching, using multimedia and other media to display content is a very suitable teaching method. Educators can use ECP for video network teaching, etc. [2]. Students can learn PE videos through ECP. To enhance the teaching effect, it is necessary to identify and predict the actions in the video. DT can extract effective information from it and

Luo, Q. (2023). Practical Analysis of Digital Technology in an Electronic Education Platform in PE Training. *International Journal of Emerging Technologies in Learning (iJET)*, 18(22), pp. 59–72. https://doi.org/10.3991/ijet.v18i22.44097

Article submitted 2023-08-19. Revision uploaded 2023-09-26. Final acceptance 2023-09-29.

perform pose matching and prediction [3]. Research has shown that OpenPose can conduct real-time educational monitoring and provide feedback to teachers on the acquired information. MC Su et al. used this method to establish a visual detection system for analyzing students' actions and behaviors. The system can effectively recognize students' facial expressions and body movements and has a small detection error [4]. However, OpenPose is highly complex and computationally difficult at runtime. Therefore, further improvements are needed in practical applications. MobileNet is an improved version of the convolutional neural network (CNN). It can be used in image processing, feature extraction, and other work. Unlike traditional CNN, MobileNet belongs to a lightweight network model, which can reduce the computational difficulty of backbone networks. Therefore, this study proposes to introduce this model to optimize OpenPose. At the same time, to ensure the accuracy of the model while improving its running speed, the experiment also introduced SAM for optimization. Deng T. et al. conducted research on the detection of road vehicles. The experimental content proves that the introduction of the attention mechanism improves the real-time feature extraction ability of the MobileNetv3 network [5]. Based on the existing achievements, this study proposes to use OpenPose for posture matching in PE teaching. MobileNet and SAM are also introduced for method optimization. It is hoped to improve the practical effect of DT in PE electronic education platform.

2 RELATED WORKS

The application of ECP can give full play to the limited teaching resources, such as teachers and venues. This approach breaks the constraints of time and space, can maximize the enrichment of students' teaching content, and further improves the quality of PE teaching. Using ECP can connect teaching resources, educators, and students [6]. The application of ECP in PE can achieve virtual teaching, intelligent teaching, precision education, and multiple teaching. DT is an important technical means for the application of ECP. The application of DT has promoted the establishment of ECP and the optimization and improvement of ECP [7]. Data processing and intelligent computing can be performed through DT in ECP. Therefore, DT can significantly improve the application of ECP in physical education. ECP contains many teaching video resources. Therefore, further research on ECP is needed. Among the resources stored on ECP, video resources are the main teaching resources. Teachers can use online teaching videos for physical education. Students can use video to imitate and connect actions. Therefore, the recognition and prediction of human motion in video have become the focus of research. At this point, the relevant DT can be used to identify and predict human actions. In existing research, OpenPose can refine and classify human bone points, etc., to achieve effective posture matching. In human gait analysis, OpenPose can detect human joint points, and it can also measure human joint angles. Through data processing, this method can be involved in human motion analysis [8]. During autonomous learning, OpenPose can accurately extract bone data from sick children and predict track movements based on this data. This method can effectively reduce data noise and has high efficiency in pose matching. This has a positive promotion effect on the treatment of sick children [9]. Some scholars have integrated OpenPose with other methods. Based on this, they established a deep learning model that can be used to detect dynamically changing behavior. This model can predict real-time changes and can be used for behavior monitoring and prediction in intelligent manufacturing [10]. Huang S. et al. used this method to

detect subway ticket evasion. This method can extract and estimate human skeleton information. The researchers then introduced a pose flow to track bone sequences. The optimized method effectively detects and estimates the final state of the human body and can be used to detect ticket evasion behavior [11].

Researchers such as Da T. have applied MobileNet to the prediction of low-resolution images and combined it with CNN to refine image information. Based on this, a lightweight image segmentation method was established in the experiment. This method can effectively perform image segmentation while maintaining high operational efficiency [12]. Tsutsumi T. et al. have shown that MobileNet can effectively process pathological images. This model can effectively distinguish between normal and abnormal images. In the model validation results, this method has high performance in distinguishing pathological images [13]. In large-scale inkjet printing work, researchers have improved MobileNetV2 and applied it to image classification. After parameter optimization and method improvement, the method can accurately predict inkjet conditions. The optimized method can successfully demonstrate the inkjet process, ensure the efficiency of the testing process, and reduce the testing time [14]. Kulkarni U. et al. used MobileNet for feature extraction of visual images. Through parameter optimization, the redundancy of the network is effectively reduced while reducing quantization losses. At the same time, while maintaining high prediction accuracy, the new model can also reduce the parameter volume and improve operational efficiency [15]. When faced with complex images, attention mechanisms can be used to extract image features. When combined with self-supervised learning methods, this method can refine the image features and obtain corresponding feature maps. The validation results in the dataset confirm that the method has high detection performance [16]. Hu J. et al. proposed that the dual attention mechanism can be used to improve image quality. Two modules were introduced to establish a dual attention mechanism to improve the feature thinning ability of defect images. MobileNet was also introduced to classify image features. The combination of the two can effectively improve the processing results of defect images, with an accuracy rate of over 98% [17]. Yue J. et al. used the lightweight MobileNet to study images of fish schools. At the same time, SAM was introduced to improve the method. Through the combination of methods, the problems of image occlusion and low image clarity were solved in the research. The improved method's detection rate results in different data sets are above 88% [18].

From the contents above, OpenPose exhibits high performance in pose matching and has a high application value. The MobileNet model not only maintains the feature extraction capabilities of traditional methods but also effectively improves efficiency. At the same time, the attention mechanism model can further improve the accuracy of feature extraction. Therefore, in this study, OpenPose was selected as a posture-matching method in PE teaching. To further improve the efficiency and accuracy of this method, MobileNet and SAM are also introduced for method optimization. It is hoped to further enhance the practical effect of DT in PE teaching.

3 PRACTICAL ANALYSIS OF DT IN PE TRAINING

3.1 A pose matching algorithm based on OpenPose

OpenPose human posture estimation can predict the joint points of the human body in video, showing strong robustness in estimating human posture. Based on OpenPose, a PE teaching system was designed. The system can use posture matching to evaluate the standard degree of basic sports movements. The entire PE teaching

system mainly includes three parts, namely, the image preprocessing module, the posture information extraction module, and the posture matching module. Firstly, in the preprocessing module, it can preprocess the PE teaching video through OpenPose to obtain the coordinates of the bone points. Then, standardization processing was carried out. After video preprocessing, it is necessary to extract gesture information from the video. It mainly includes the acquisition of center of gravity information, limb angle information, and human upward information. Then the different posture features are fused. The next step is gesture matching. It mainly includes posture matching evaluation, deviation limb recognition, and deviation limb identification. Through this sports teaching system, it is possible to evaluate whether students' sports training actions are standard, which is conducive to improving the quality of students' sports teaching. Figure 1 shows the module display of the PE teaching system.

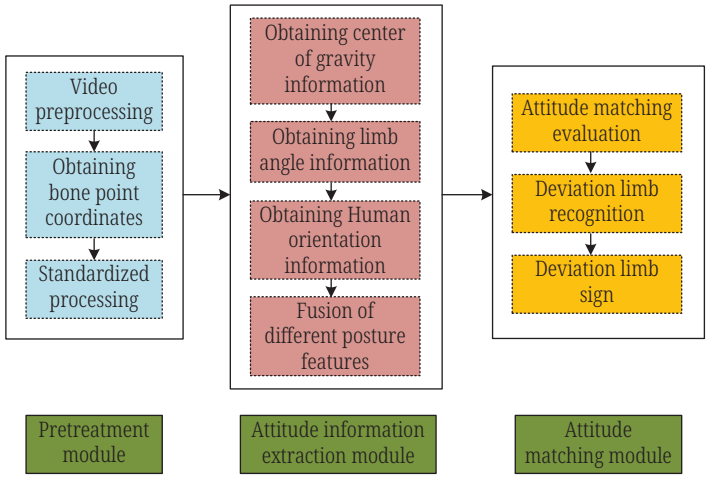

Fig. 1. Module display of PE teaching system

OpenPose is the key technology of the entire PE teaching system, so this experiment describes this method in detail. OpenPose is a human bone point prediction model built on the basis of CNN. It can predict bone points by constructing CNN in stages while outputting its predicted confidence heat map. Affinity fields (AFs) are the basis for connecting different skeletons. To improve the accuracy and speed of model prediction, OpenPose predicts AFs between different points and predicts the bone points in the next stage. Figure 2 shows the network architecture of OpenPose.

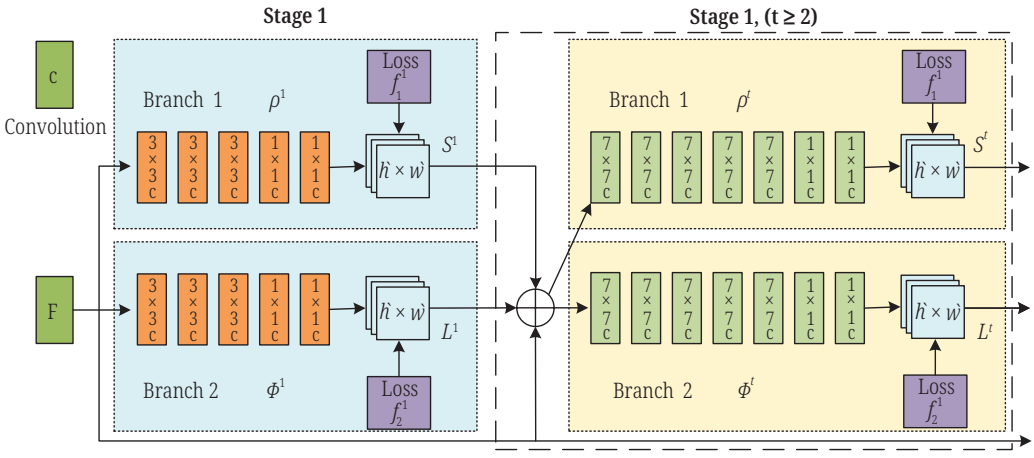

Fig. 2. Network architecture of OpenPose

The main backbone network of CNN is VGG-19. In OpenPose's network architecture, it is necessary to initialize and fine-tune the top 10 network layers in the VGG-19 structure. From this, a set of input characteristics can be obtained. Then map them to the first level of the branch, respectively. In the first phase of the OpenPose network architecture, part of the AFs field $L^t = \varnothing^1(F)$ and detection confidence diagram $S^1 = \rho^1(F)$ are generated. Where F represents the mapping, and $\varnothing^1$ and ρ^1 represent the CNN used for reasoning. In the subsequent stages, the confidence diagram for stage t can be obtained using formula (1).

$$S^t = \rho^t(F, S^{t-1}, L^{t-1}), \forall t \geq 2 \tag{1}$$

$\varnothing^1$ and ρ^t represent the CNN used for reasoning in the t stage in formula (1). Then, partial AFs fields of stage t can be obtained using formula (2).

$$L^t = \varnothing^t(F, S^{t-1}, L^{t-1}), \forall t \geq 2 \tag{2}$$

At the end of the different stages, each branch uses a loss function. This loss function can guide the model to predict limb AFs in S^1 and branch 2. At the same time, the regularization term in the experiment selects the L2 norm and uses it to spatially weight the loss function. Equation (3) is the loss function of the first branch at stage t. Equation (4) is the loss function of the second branch at stage t.

$$f_L^t = \sum_{j=1}^{J} \sum_{p} W(p) \cdot \left\| S_j^t(p) - S_j^*(p) \right\|_2^2 \tag{3}$$

$$f_L^t = \sum_{c=1}^{C} \sum_{p} W(p) \cdot \left\| L_c^t(p) - L_c^*(p) \right\|_2^2 \tag{4}$$

In equations (3) and (4), p represents the learning position. The confidence graph and partial affinity vector field of labeled nodes are represented as S_j^* and L_c^*, respectively. When the binary mask matches the $W(p) = 0$, W can avoid affecting the true prediction. To avoid the occurrence of gradient disappearance problems at different stages, periodic gradient supplementation can be carried out. This process requires intermediate supervision. During the training process, equation (5) represents the overall training goal.

$$f = \sum_{t=1}^{T} (f_S^t + f_L^t) \tag{5}$$

3.2 Pose matching algorithm based on improved OpenPose

The above section provides a basic description of the principles of OpenPose network architecture. In the established PE teaching system, OpenPose has high accuracy. However, in practical applications, the model structure based on the OpenPose network architecture is relatively complex. This results in a large amount of calculation, a long running time, and a huge consumption of storage space for the model. Therefore, further optimization and streamlining of OpenPose are also needed to compress the running time of the algorithm. It is proposed to introduce the MobileNetv3 lightweight network to replace the VGG-19 network structure applied in the OpenPose network architecture. MobileNetv3 network architecture is also a type of CNN, but this network architecture can significantly reduce the amount of computation and the volume of parameters. MobileNetv3 is mainly divided into a

deep convolution layer (DCL), an inverted residual structure (IRS), a point-wise convolution layer (PCL), and a channel attention SE module. Figure 3 shows the network structure of MobileNetv3.

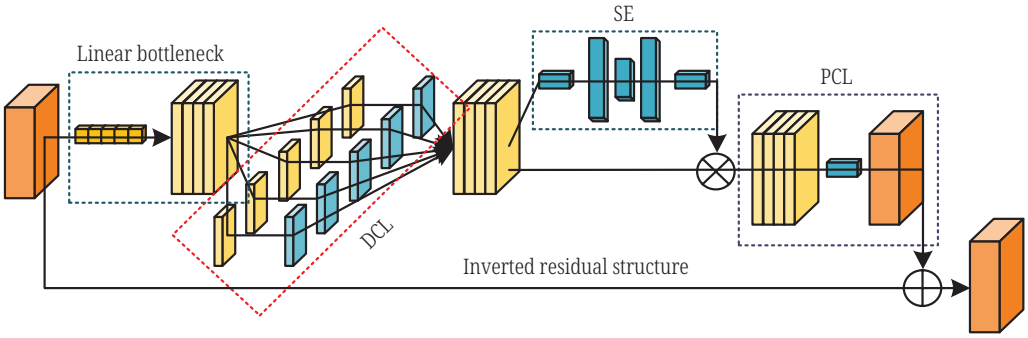

Fig. 3. Network structure of MobileNetv3

In the MobileNetv3 network architecture, DCL and PCL can be combined to perform deeply separable convolution operations. This is why MobileNetv3 can reduce the amount of computation and parameter volume. At the same time, in the MobileNetv3 network architecture, a PCL, the linear bottleneck architecture, is placed at the forefront. In adjacent modules, the number of deep convolution kernels located at adjacent input locations is easily limited. The linear bottleneck structure can solve this problem. Assume that the input characteristic graph in the MobileNetv3 network structure is F_{input}. Equation (6) provides the expression.

$$F_{input} \in \Re^{H_{in} \times W_{in} \times C_{in}} \tag{6}$$

In equation (6), H_{in} is the height of the feature map, W_{in} means the width of the feature map, and C_{in} represents the number of channels in the feature map. Equation (7) is a traditional convolutional kernel expression.

$$F_{input} \in \Re^{H_k \times W_k \times C_{in} \times N} \tag{7}$$

In equation (7), H_k is convolution kernel's height, W_k means convolution kernel's width, C_{in} refers to convolution kernel's channels number, and N represents convolution cores number. Equation (8) presents an output characteristic graph with a channel number of N.

$$F_{output} \in \Re^{H_{out} \times W_{out} \times N} \tag{8}$$

In equation (8), H_{out} represents output characteristic graph's height, and W_{out} means output characteristic graph's width. Equation (9) provides a calculation method for point convolution kernels.

$$K_{PC} \in \Re^{1 \times 1 \times C_{in} \times N} \tag{9}$$

Point convolution cores are the key to solving the problem of limited number of deep convolution cores in MobileNetv3 network architecture. Equation (10) is a calculation method for the point depth convolution kernel.

$$K_{DC} \in \Re^{H_k \times W_k \times C_{in}} \tag{10}$$

The dimension size of the deep convolution kernel is consistent with that of the traditional convolution kernel. The difference between deep convolution and traditional convolution is that deep convolution has the same size of output and input channels. Through the above definition, by using the calculation method, the amount C and the parameter volume S in traditional convolution can be obtained. Equation (11) is the calculation method for C.

$$C = \sum_{n=1}^{N}\sum_{c=1}^{C_{in}}\sum_{h=1}^{H_{out}}\sum_{w=1}^{W_{out}}(H_k \times W_k) \tag{11}$$

Equation (12) is the calculation method of S.

$$S = \sum_{n=1}^{N}\sum_{c=1}^{C_{in}}(H_k \times W_k) \tag{12}$$

By using the calculation method amount C_d and the parameter volume S_d in depth convolution can be obtained. Equation (13) is the calculation method for C_d.

$$C_d = \sum_{c=1}^{C_{in}}\sum_{h=1}^{H_{out}}\sum_{w=1}^{W_{out}}(H_k \times W_k) + \sum_{n=1}^{N}\sum_{c=1}^{C_{in}}(H_{out} \times W_{out}) \tag{13}$$

Equation (14) is the calculation method for Sd.

$$C_d = \sum_{c=1}^{C_{in}}((H_k \times W_k) + (N \times C_{in})) \tag{14}$$

From equations (11) to (14), the C_d and S_d in deep convolution are greatly reduced, which improves the running speed of MobileNetv3. However, this can also lead to a loss of recognition accuracy. Therefore, to ensure the running speed of MobileNetv3 while improving its recognition accuracy, a channel domain SE module is introduced into the structure. This can increase the amount of channel information and improve the network's representation ability. To a certain extent, the introduction of the SE module improves recognition accuracy. However, for the complex environment in sports teaching videos, the structure still needs to be further optimized. Therefore, in this study, the spatial domain SAM was also introduced, and the self-attention SE module was generated. Figure 4 shows the structure of the self-attention mechanism.

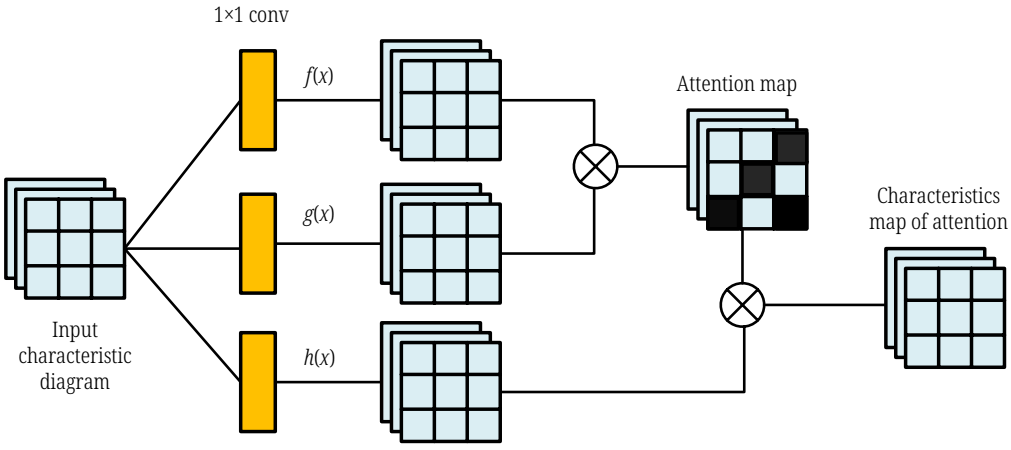

Fig. 4. Structural diagram of the self-attention mechanism

As illustrated in Figure 4, there are mainly three parts of SAM. Firstly, it is necessary to input the feature map obtained in MobileNetv3 into three convolution modules, so as to obtain a triple (Q, K, V) of the feature map. The calculation of similarity can be obtained using the dot product of Q and K. The calculated result is then divided by $\sqrt{d_k}$, where d_k is the dimension of Q and K. Then, the Softmax function is used to process the results. Finally, the obtained results are weighted and summed with V. See equation (15) for specific calculation

$$Attention(Q,K,V) = soft\max\left(\frac{QK^T}{\sqrt{d_k}}\right)V \tag{15}$$

In addition, the feature map of the output was compressed and activated in the study. Compression operations can obtain global information. The activation operation can have the importance of obtaining inter-channel information. The above operations can greatly reduce the calculation amount and parameter volume. The final feature weights can be calculated using the sigmoid activation function, achieving the goal of recalibrating features. In the channel domain and the spatial domain, after obtaining the new weight distribution, the attention modules of these two dimensions are introduced into the OpenPose network structure in a parallel manner, enabling it to learn more features. After obtaining the features, it is necessary to go through the initialization and refinement stages to obtain partial AFs and key-point heat maps. That is, in the OpenPose network structure, two branches are applied at different prediction stages. At the same time, the weights of the previous layers in the network structure are shared to obtain a single prediction branch. This can reduce the amount of calculation.

4 VALIDATION ANALYSIS OF DT IN PE TRAINING

To ensure the objectivity and comparability of the validation analysis, all operations during the validation process are performed in the same hardware and software environment. The operating system used in the verification experiment is Windows 10, the GPU hardware is GeForce 2080Ti, and the RAM is 4.00G. The version of the application software is MATLAB R2013B. The data set used for the validation test is the COCO data set, and the data in this data set is highly representative and comprehensive. There are 1000 sets of data used for validation. The ratio of the training set to the test set in the data is 9:1. After initial testing and debugging, the parameter settings of the algorithm were determined. The proposed algorithm and the comparison algorithm use the same settings to ensure comparability. The initial learning rate and decay ratio of the algorithm are both 0.1. During training, Adam optimization was used to improve algorithm performance (see Table 1).

Table 1. Experimental environment

System	Windows 10	Graphics card	GeForce 2080Ti
Software	MATLAB R2013B	RAM	4.00G
Data Set	COCO	Deep learning framework	Pytorch 1.7.1
Picture Size	224,416,512	Batch size	8,16,32
Optimizer During Training	Adam	Initial learning rate	0.1
Decay Period	5	Decay ratio	0.1

The important indicators for evaluating the effectiveness of model training are the loss function and mean square error (MSE). The faster these two indicators decrease with the increase in the number of iteration steps and the lower the value after stabilization, the better the effectiveness of model training. To verify the value of the proposed algorithm, current algorithms of the same kind, OpenPose, MobileNetv3+self, and MobileNetv3+SE, are compared. Figure 5 shows the statistical results of the loss function and MSE evaluation indicators. Figure 5a shows the loss function, and Figure 5b shows the MSE. It was observed that the two indicators of the proposed algorithm decreased the fastest. When iteration step number is 20, the proposed algorithm's loss function value is 0.242, and MSE is 0.573. Under the same iteration steps, other algorithms' performance is worse than the proposed algorithm. When the iteration reaches 120 steps, the curves of all algorithms tend to be stable. At this time, the two index values of the proposed algorithm are still the lowest, but all algorithms have a small difference.

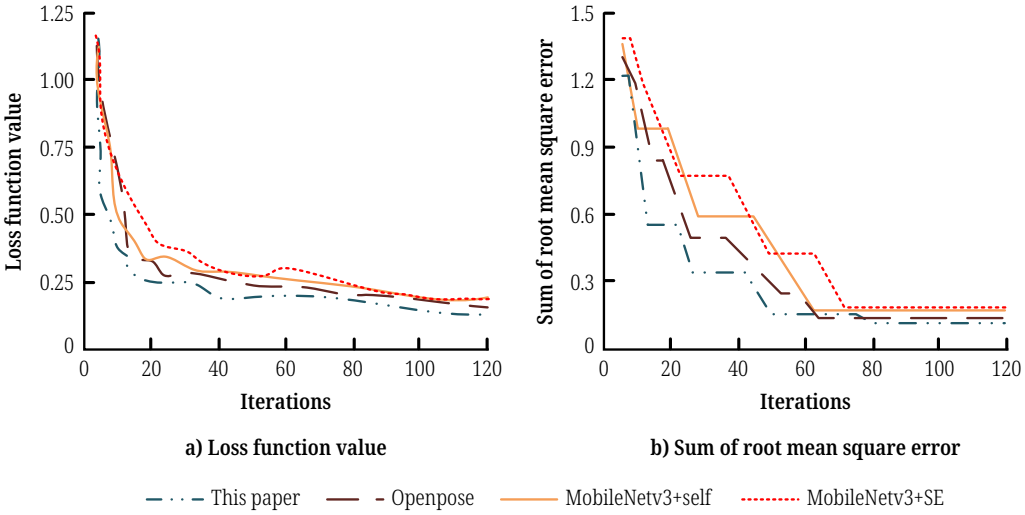

Fig. 5. Loss function and sum of root mean square error

After evaluating the training results, the test results can be evaluated. The model training quality plays a decisive role in algorithm performance. Figure 6 shows the mean absolute error (MAE) and root mean square error (RMSE) indicators under the test set. These two indicators show the algorithm's error situation from different perspectives. The fewer algorithm errors, the stronger the algorithm's performance. Figure 6a shows MAE indicator test results, and Figure 6b shows RMSE indicator test results. In the test set, the MAE and RMSE curves of the proposed algorithm are generally stable, indicating fluctuations in a small range. The differences in error situations can be intuitively seen from the curves of each algorithm. Under both indicators, the error curve of the proposed algorithm is at the bottom, representing the lowest overall error. After calculation, the proposed algorithm has a mean MAE of 0.793 and a mean RMSE of 0.628, both of which are the lowest among the algorithms. The training results of the algorithm are good, and the algorithm shows the lowest error in testing.

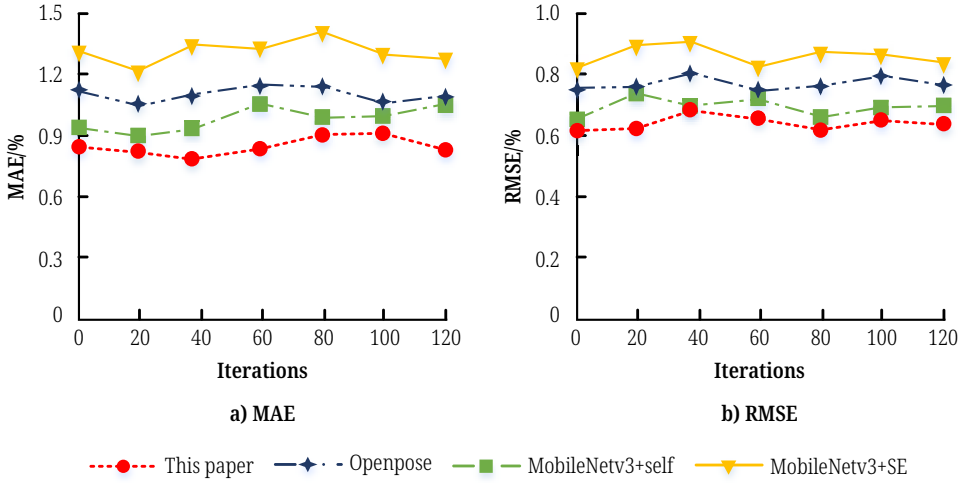

Fig. 6. MAE and RMSE of different models

Table 2 shows the evaluation results of the indicators used to evaluate algorithm performance, in addition to error. To verify the performance of each algorithm in different environments, they were tested at image sizes of 224, 416, and 512, respectively. The accuracy rate of the proposed algorithm under 224 image sizes is 0.887, the recall rate is 0.571, and the F1 value is 0.408. As the image size increases, the above indicators of the proposed algorithm also increase. Comparing different algorithms under the same image size, the proposed algorithm's relevant indicators are always the highest. When image size is 416, the proposed algorithm's accuracy rate is 0.989, and the closest one to it is the MobileNetv3+self-algorithm, with an accuracy value of 0.887. Other algorithms' accuracy rates are lower than this value. These algorithms all have significant fluctuations depending on the image size, but the overall performance of the proposed algorithm is steadily higher than other algorithms.

Table 2. Performance indicators comparison

Model	Image Size	Mean Average Precision	Precision	Recall	F1
This paper	224	0.867	0.887	0.571	0.408
	416	0.949	0.989	0.673	0.500
	512	0.969	0.979	0.765	0.510
OpenPose	224	0.734	0.765	0.510	0.326
	416	0.816	0.847	0.571	0.357
	512	0.857	0.867	0.612	0.408
MobileNetv3+self	224	0.816	0.816	0.581	0.398
	416	0.857	0.887	0.612	0.408
	512	0.918	0.949	0.663	0.459
MobileNetv3+SE	224	0.602	0.632	0.388	0.296
	416	0.683	0.694	0.469	0.326
	512	0.765	0.796	0.510	0.377

Accuracy is one of the most intuitive and important evaluation indicators of an algorithm, which directly reflects the algorithm's ability to correctly process target data. Figure 7 shows the accuracy and performance of each algorithm in training and

test sets. Figure 7a shows algorithm performance when training. Figure 7b shows algorithm performance when tested. Observing the curve shape, the proposed algorithm's accuracy is the highest in both training and testing. Each algorithm exhibits significant fluctuations in the test set, while its curve in the training set is relatively smooth. This is caused by the algorithm's nature itself. In the test set, the algorithm's accuracy rate reached a maximum of 0.893, and its accuracy rate throughout the entire operation process is always higher than that of other comparison algorithms. In the training set, the proposed algorithm's accuracy rate is up to 90%, indicating that this algorithm's performance in training and testing is relatively close.

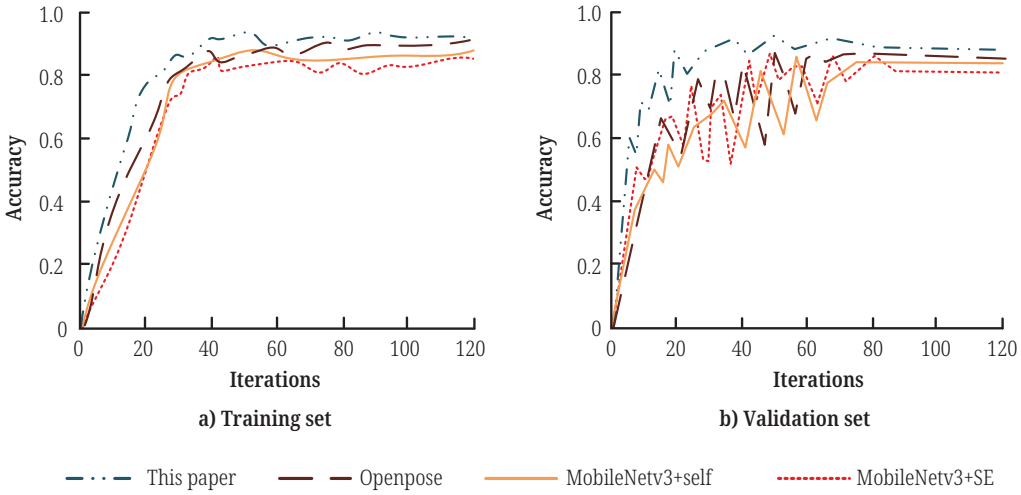

Fig. 7. Accuracy of different data set

To conduct a more comprehensive evaluation of the algorithm, relevant data were also collected, and the receiver operating characteristic (ROC) curves of each algorithm were plotted during the validation process. This orientation takes specificity and sensitivity as the coordinate axes and visualizes algorithm performance. From a graphical perspective, the larger the area under the curve, the better the algorithm's performance. Figure 8 shows the ROC curves of each algorithm. Overall, the proposed algorithm has the largest area under the curve, which represents a better overall performance of the proposed algorithm. For a more intuitive analysis, by zooming in on some of the spaces in the figure, the proposed algorithm's ROC curve is smoother, while the other three comparative algorithms have significant fluctuations in some positions.

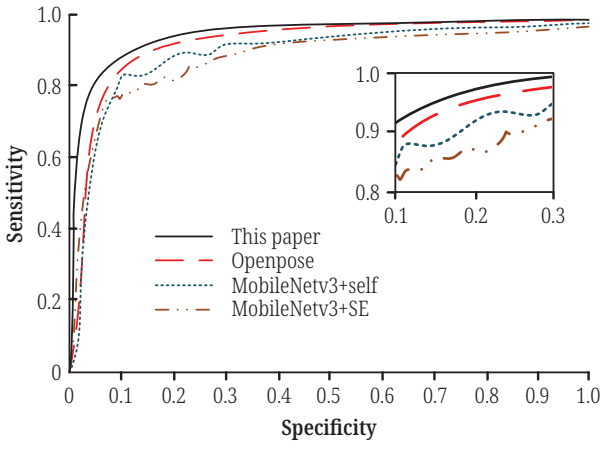

Fig. 8. ROC curve results in COCO data set

The final step in verification is to test algorithm performance in real sports training. The proposed algorithm is applied to real sports training. Its output and the real situation's difference are observed. Figure 9 shows the validation results. Figure 9a shows the algorithm's comparison between calculated results and actual values. Figure 9b shows their relative and absolute errors. The difference between the actual long jump scores and the system test scores under different test numbers is small. The absolute error between the algorithm results and the true value under each number does not exceed 1.5 cm, while the relative error does not exceed 1.2%. The minimum absolute error and relative error are 0.01 cm and 0.2%, respectively. This result demonstrates the application value of the algorithm in practical sports training.

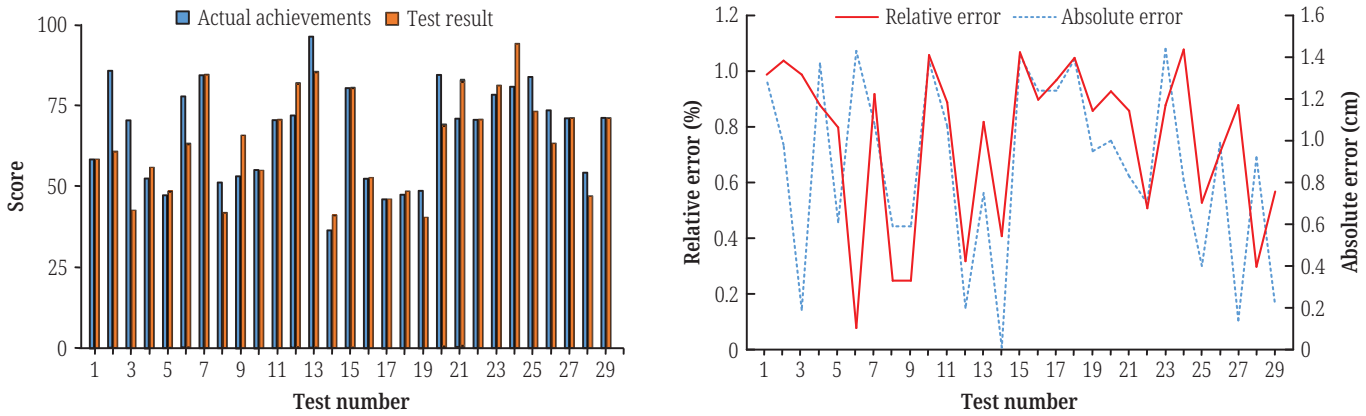

a) Comparison between actual test results and system test results

b) Comparison of error results between actual test scores and system test scores

Fig. 9. Comparison of scores and error results between actual long jump results and test results

5 CONCLUSIONS

In the ECP of PE, the application of DT has promoted the development of physical education. To better improve the application effect of DT in physical education, this study proposes using Open Pose as a posture matching method in physical education. To further improve the efficiency and accuracy of this method, Mobile Net and SAM are also introduced for method optimization. In performance verification results, the proposed algorithm has a mean MAE of 0.793 and a mean RMSE of 0.628. When tested, the proposed algorithm's highest accuracy rate was 0.893. When training, the proposed algorithm's accuracy rate is up to 90%. This algorithm's ROC curve is smoother and has the largest area. In practice of PE, the actual long jump score and system test score's difference is small. The algorithm's results and true value's absolute error do not exceed 1.5 cm under each number, while its relative error does not exceed 1.2%. The minimum absolute error and relative error are 0.01 cm and 0.2%, respectively. The proposed algorithm has a high prediction effect and performance and can be applied to PE teaching. However, this method has not yet been applied to more complex sports action teaching. The impact of complex environments on this method has not been studied. In subsequent experiments, it is also necessary to consider complex actions and scenarios' impacts.

6 FUNDINGS

The research is supported by Subject of Hunan Provincial Bureau of Sports: The media logic and construction path of Olympic culture in shaping the values of young people in the new era (No.: 2022XH019); Scientific research project of Hunan Province: Research on the path of social forces supporting public sports services in rural areas of Hunan Province in the context of the common prosperity strategy (No.: 22C1091).

7 REFERENCES

[1] J. Abraham and S. Geobey, "Digital elixir? The Aakash tablet as a social innovation in information and communication technology for development (ICT4D)," *Social Enterprise Journal*, vol. 18, no. 2, pp. 288–305, 2022. https://doi.org/10.1108/SEJ-12-2020-0133

[2] A. Mujalli and A. T. Khan, "Almgrashi university accounting students and faculty members using the blackboard platform during COVID-19; proposed modification of the UTAUT model and an empirical study," *Sustainability*, vol. 14, no. 4, pp. 2360–2377, 2022. https://doi.org/10.3390/su14042360

[3] Z. He, Y. Wang, X. Qin, R. Yin, Y. Qiu, K. He, and Z. Zhu, "Classification of neurofibromatosis-related dystrophic or no dystrophic scoliosis based on image features using Bilateral CNN," *Medical Physics*, vol. 48, no. 4, pp. 1571–1583, 2021. https://doi.org/10.1002/mp.14719

[4] M. C. Su, C. T. Cheng, M. C. Chang, and Y. Z. Hsieh, "A video analytic in-class student concentration monitoring system," *IEEE Transactions on Consumer Electronics*, vol. 67, no. 4, pp. 294–304, 2021. https://doi.org/10.1109/TCE.2021.3126877

[5] T. Deng and Y. Wu, "Simultaneous vehicle and lane detection via MobileNetV3 in car following scene," PLoS ONE, vol. 17, no. 3, pp. 1–18, 2022. https://doi.org/10.1371/journal.pone.0264551

[6] A. Huseynova and A. Mazanova, "The state of application of electronic education system in Azerbaijan," *Turkish Journal of Computer and Mathematics Education (TURCOMAT)*, vol. 12, no. 6, pp. 1247–1254, 2021. https://doi.org/10.17762/turcomat.v12i6.2464

[7] A. W. Khurniawan and Erda G. Irmawaty, "A second order confirmatory factor analysis of the digital transformation for a distance education institution," *International Journal of Education and Practice*, vol. 10, no. 4, pp. 381–392, 2022. https://doi.org/10.18488/61.v10i4.3224

[8] M. Ota, H. Tateuchi, T. Hashiguchi, and N. Ichihashi, "Verification of validity of gait analysis systems during treadmill walking and running using human pose tracking algorithm," *Gait & Posture*, vol. 85, pp. 290–297, 2021. https://doi.org/10.1016/j.gaitpost.2021.02.006

[9] Y. Zhang, Y. Tian, P. Wu, and D. Chen. "Application of skeleton data and long short-term memory in action recognition of children with autism spectrum disorder," *Sensors*, vol. 21, no. 2, pp. 411–427, 2021. https://doi.org/10.3390/s21020411

[10] X. Zhou, X. Xu, W. Liang, Z. Zeng, S. Shimizu, L. T. Yang, and Q. Jin, "Intelligent small object detection for digital twin in smart manufacturing with industrial cyber-physical systems," *IEEE Transactions on Industrial Informatics*, vol. 18, no. 2, pp. 1377–1386, 2022. https://doi.org/10.1109/TII.2021.3061419

[11] S. Huang, X. Liu, W. Chen, G. Song, Z. Zhang, L. Yang, and B. Zhang, "A detection method of individual fare evasion behaviours on metros based on skeleton sequence and time series," *Information Sciences*, vol. 589, no. 1, pp. 62–79, 2022. https://doi.org/10.1016/j.ins.2021.12.088

[12] T. Da and L. Yang, "TextureMask: A merged architecture for low-resolution instance segmentation," *Intelligent Data Analysis*, vol. 25, no. 4, pp. 993–1012, 2021. https://doi.org/10.3233/IDA-205250

[13] K. Tsutsumi, K. Goshtasbi, A. Risbud, P. Khosravi, and M. Abouzari, "A web-based deep learning model for automated diagnosis of otoscopic images," *Otology & Neurotology*, vol. 42, no. 9, pp. E1382–E1388, 2021. https://doi.org/10.1097/MAO.0000000000003210

[14] Eunsik Choi Kunsik, An, and Kyung-Tae Kang, "Deep-learning-based microfluidic droplet classification for multijet monitoring," *ACS Applied Materials & Interfaces*, vol. 14, no. 13, pp. 15576–15586, 2022. https://doi.org/10.1021/acsami.1c22048

[15] U. Kulkarni, S. M. Meena, S. V. Gurlahosur, and G. Bhogar, "Quantization Friendly MobileNet (QF-MobileNet) architecture for vision based applications on embedded platforms," *Neural Networks*, vol. 136, no. 1, pp. 28–39, 2021. https://doi.org/10.1016/j.neunet.2020.12.022

[16] M. Tian, Y. Cui, H. Long, and J. Li, "Improving novelty detection by self-supervised learning and channel attention mechanism," *Industrial Robot*, vol. 48, no. 5, pp. 673–679, 2021. https://doi.org/10.1108/IR-10-2020-0241

[17] J. Hu, P. Yan, Y. Su, D. Wu, and H. Zhou, "A method for classification of surface defect on metal workpieces based on twin attention mechanism generative adversarial network," *IEEE Sensors Journal*, vol. 21, no. 12, pp. 13430–13441, 2021. https://doi.org/10.1109/JSEN.2021.3066603

[18] J. Yue, H. Yang, S. Jia, Q. Wang, Z. Li, G. Kou, and R. Ba, "A multi-scale features-based method to detect Oplegnathus," *Information Processing in Agriculture*, vol. 8, no. 3, pp. 437–445, 2021. https://doi.org/10.1016/j.inpa.2020.10.001

8 AUTHOR

Qiyu Luo, male, born in February 1966 in Yiyang, Hunan Province, bachelor's degree, is now the deputy secretary of the Party Committee and president of Hunan Sports Vocational College (E-mail: Qiyu_Luo@outlook.com).